



A CRISPR-Cas9 screen identifies mitochondrial translation as an essential process in latent KSHV infection of human endothelial cells

Daniel L. Holmes^a , Daniel T. Vogt^a , and Michael Lagunoff^{a,1}

^aDepartment of Microbiology, University of Washington, Seattle, WA 98109

Edited by Donald E. Ganem, Novartis Institutes for Biomedical Research, Inc., Emeryville, CA, and approved September 30, 2020 (received for review June 9, 2020)

Kaposi's sarcoma-associated herpesvirus (KSHV) is the etiologic agent of Kaposi's sarcoma (KS) and primary effusion lymphoma (PEL). The main proliferating component of KS tumors is a cell of endothelial origin termed the spindle cell. Spindle cells are predominantly latently infected with only a small percentage of cells undergoing viral replication. As there is no direct treatment for latent KSHV, identification of host vulnerabilities in latently infected endothelial cells could be exploited to inhibit KSHV-associated tumor cells. Using a pooled CRISPR-Cas9 lentivirus library, we identified host factors that are essential for the survival or proliferation of latently infected endothelial cells in culture, but not their uninfected counterparts. Among the many host genes identified, there was an enrichment in genes localizing to the mitochondria, including genes involved in mitochondrial translation. Antibiotics that inhibit bacterial and mitochondrial translation specifically inhibited the expansion of latently infected endothelial cells and led to increased cell death in patient-derived PEL cell lines. Direct inhibition of mitochondrial respiration or ablation of mitochondrial genomes leads to increased death in latently infected cells. KSHV latent infection decreases mitochondrial numbers, but there are increases in mitochondrial size, genome copy number, and transcript levels. We found that multiple gene products of the latent locus localize to the mitochondria. During latent infection, KSHV significantly alters mitochondrial biology, leading to enhanced sensitivity to inhibition of mitochondrial respiration, which provides a potential therapeutic avenue for KSHV-associated cancers.

KSHV | HHV-8 | mitochondria | Crispr/Cas9 | Kaposi's sarcoma

Kaposi's sarcoma (KS) predominately arises in the context of immune suppression in the developed world but not in sub-Saharan Africa, where KS is common in both HIV-positive and -negative patients (1). While antiretroviral therapy eliminates KS in many patients with AIDS, not all cases are resolved. KS tumors are complex, highly vascularized lesions whose primary proliferating component is the spindle cell, a cell that expresses markers of endothelium. The majority of spindle cells are latently infected with Kaposi's sarcoma-associated herpesvirus (KSHV), with just a small percentage of cells expressing lytic transcripts (2). Herpesvirus infections are classically treated with nucleoside analogs, but this has not been effective for KS treatment, presumably because cellular latency is the predominant state of the virus in the tumor cells. Traditional chemotherapeutics are effective in some patients, but their toxicity and inaccessibility mean they are of limited use in settings with limited resources where KSHV is more prevalent (1). Therefore, a comprehensive examination of the cellular processes that are essential for infected cells has utility in identifying gene products that can be targeted with existing, accessible therapies.

Cultured human endothelial cells infected with KSHV recapitulate the proportion of latent and lytic cells seen within

KS tumors, providing a culture model for KSHV latency in tumors (3). Using cell culture systems, our laboratory has identified several cellular pathways, which can be used to selectively target latently infected cells in vitro (4–7). Recently developed lentivirus-encoded CRISPR-Cas9-based screening platforms have enabled large-scale interrogation of so-called “Achilles” genes within a population of human cells (8). These screens can be used to identify factors that are essential to the survival of cancer cells. Similar approaches have been used to identify genes that are critical for the survival of B cell lymphomas infected with Epstein-Barr virus (EBV) (9). Another important study identified genes critical for survival of primary effusion lymphoma (PEL) cells (10). PELs are a non-Hodgkin's B-cell lymphoma which maintain latent KSHV infection. All PELs are infected with KSHV but a subset of cases are also infected with EBV. While many interesting genes were identified and the study was able to compare EBV-positive with EBV-negative PEL cells, it lacked a true uninfected control for KSHV. Another study utilized KSHV-infected rat mesenchymal embryonic stem cells (11) to identify genes important for KSHV transformation in this rat cell system. However, to date no CRISPR-Cas9 essentiality screens have been performed in a human cell type relevant to KS spindle cells with mock-infected controls. To identify host factors that are required for survival and proliferation of latently infected endothelial cells, we performed a genome-wide CRISPR-Cas9 screen in human tert-immortalized microvascular endothelial (TIME) cells.

Significance

Kaposi's sarcoma-associated herpesvirus (KSHV) is the causative agent of Kaposi's sarcoma, one of the most common neoplasms in sub-Saharan Africa. There is no direct treatment for the latent state of the virus in tumors. Therefore, we sought to identify host cell targets essential to support proliferation and survival of cells latently infected with KSHV. A genome-wide CRISPR-Cas9 knockout screen to test the requirement of all human genes during KSHV latency identified host factors involved in mitochondrial translation as necessary for proliferation of latently infected endothelial cells. Antibiotics targeting bacterial ribosomes are able to selectively inhibit the proliferation of KSHV latently infected cells. Our findings provide insights into the essential function of mitochondria during latent KSHV infection.

Author contributions: D.L.H. and M.L. designed research; D.L.H. and D.T.V. performed research; D.L.H. and M.L. analyzed data; and D.L.H. and M.L. wrote the paper.

The authors declare no competing interest.

This article is a PNAS Direct Submission.

Published under the [PNAS license](#).

¹To whom correspondence may be addressed. Email: lagunoff@uw.edu.

This article contains supporting information online at <https://www.pnas.org/lookup/suppl/doi:10.1073/pnas.2011645117/-DCSupplemental>.

First published October 29, 2020.

Our screen produced 146 gene targets, which were depleted in the KSHV-infected population relative to mock controls. Many of the hits encode proteins that are known to localize to the mitochondria, and further analysis of this subset revealed mitochondrial translation to be the predominant function of these genes. Importantly, the mitochondrial ribosome has a shared ancestry with the bacterial ribosome. We found that antibiotics targeting either the large or small subunit of bacterial ribosomes and therefore, the mitochondrial ribosome can strongly suppress cell proliferation in infected endothelial cells as compared with treated mock-infected controls and also potentially induce cell death in KSHV-infected B cell lymphomas. Suppression of respiration directly, either chemically or by removal of mitochondrial genomes, produces a similar defect in cellular proliferation specifically in latently infected cells. We found changes in the mitochondrial network of cells during KSHV infection, where mitochondria become larger and longer but are fewer in number, which is consistent with but not definitive evidence of increased mitochondrial fusion. Mitochondrial transcript levels as well as mitochondrial genome copy numbers were increased during

latent infection. Interestingly, we found that multiple latent proteins localize, at least partially, to mitochondria, suggesting that more than one may be needed to sensitize cells to inhibition of mitochondrial translation.

Results

CRISPR-Cas9 Pooled Lentivirus Screen in TIME Cells during Latent KSHV Infection. To determine the host factors required for cells latently infected with KSHV to proliferate and survive, we used half of the Human Activity-Optimized CRISPR-Cas9 lentivirus library to generate a mutant pool of cells containing single guide RNA (sgRNA) and Cas9-expressing lentiviruses targeting 18,166 human genes with five sgRNAs each (Fig. 1A); ~150 million cells were transduced at a multiplicity of infection (MOI) of 0.6 and 2 d later, were placed under selection with puromycin for 3 d, the time by which a control flask of nontransduced TIME cells was completely killed. The cells were grown out for an additional 2 d and then split into two sets of flasks, each representing approximately 1,000-times coverage of the lentiviral library in 90 million cells. After the cells were settled, half were

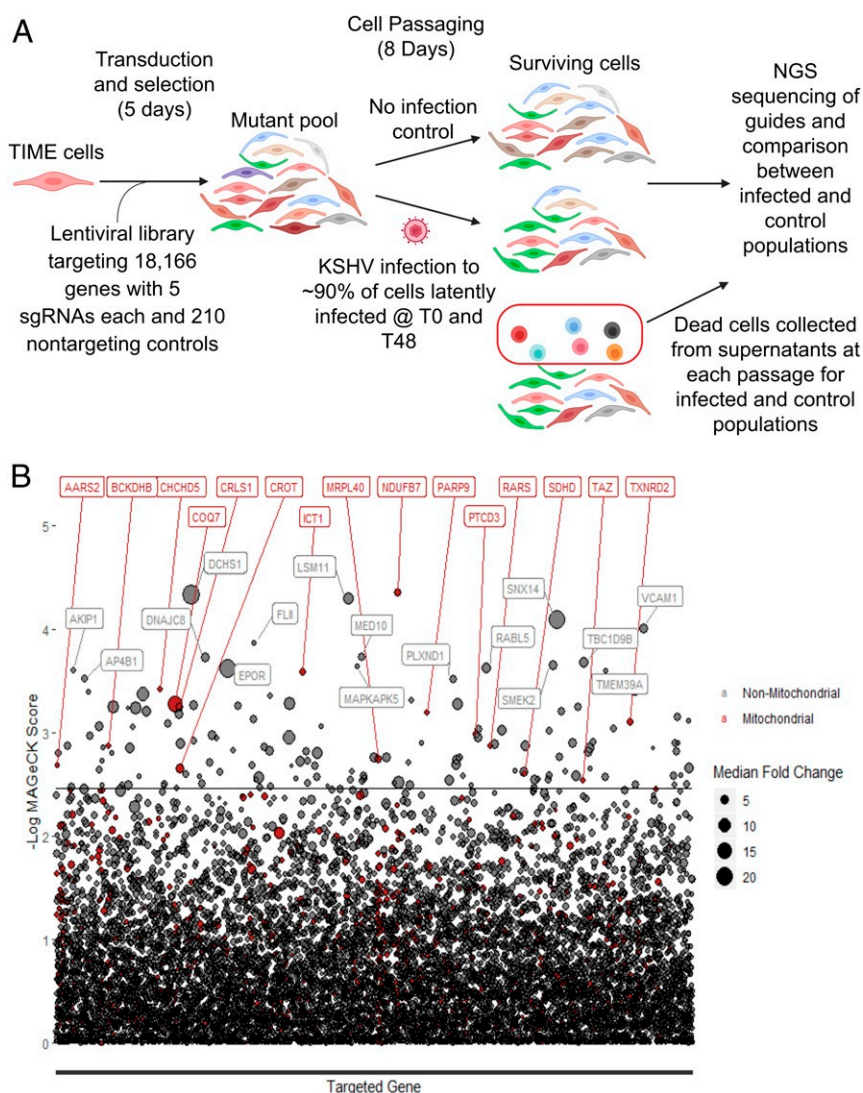


Fig. 1. CRISPR-Cas9 whole-genome screen to identify essential host factors during KSHV infection of endothelial cells. (A) Schematic of TIME cell whole-genome screen of KSHV-infected cells (T0 and T48 refer to zero and 48 hours post initial KSHV infection, respectively. NGS stands for next generation sequencing). (B) Plot of the results of the live cell screen. The back line represents the false discovery rate cutoff of 0.25. The size of the circles represents the magnitude of the median log fold change for all sgRNAs for that particular gene. All red circles accompanied by red text are genes whose gene products localize to mitochondria.

infected with KSHV obtained from induction of body cavity-based lymphoma-1 (BCBL1) cells; 2 d later, these cells were reinfected with KSHV to ensure that infection rates remained sufficiently high for the remainder of the experiment. After the second infection, 91% of cells stained positive for latency associated nuclear antigen (LANA), a marker of KSHV latency. For 8 d, the cells were passaged, splitting to maintain representation of the library. At each passage, the dead cells in the supernatant of both the control and KSHV-infected samples were pelleted. At the end of 8 d, the live cells were harvested. Genomic DNA was harvested from the live cell samples as well as the dead cell samples, and next-generation sequencing libraries were prepared and sequenced. sgRNA abundances were calculated by mapping sequencing reads to the library, and the changes in representation of guides targeting different genes between infected and uninfected samples were determined using MAGeCK (12). sgRNAs depleted in the live cells infected with KSHV relative to

the uninfected population as well as sgRNAs enriched in the dead cells infected with KSHV relative to uninfected were identified (Fig. 1B and *SI Appendix*, Fig. S1); 146 genes (*SI Appendix*, Table S1) were significantly depleted from the live cell population of latently infected TIME cells as compared with the uninfected TIME cells using a false discovery rate cutoff of 0.25 (*Dataset S1*). Interestingly, sgRNAs for two genes, KCTD10 and HSPA4, were significantly enriched in KSHV-infected cells, suggesting these genes selectively suppress growth during KSHV infection; 1,600 genes were enriched in the dead cell population by greater than 2.75-fold median log fold change across sgRNAs for each gene when comparing the infected cells with the uninfected cells (*Dataset S2*).

Components of the Mitochondrial Translation Machinery Are Essential for Latent KSHV Infection. Approximately 10% of the genes depleted from our live cell screen encode proteins that localize

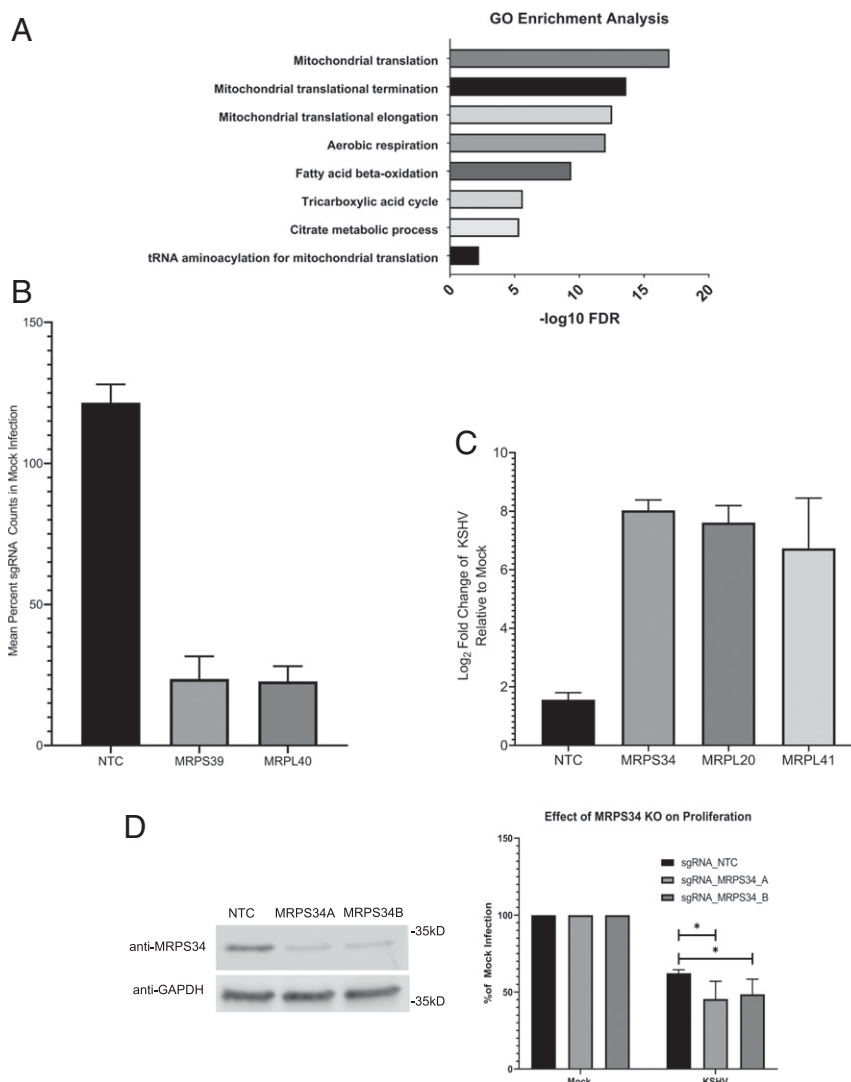


Fig. 2. Genes involved in mitochondrial translation are essential during KSHV infection. (A) Gene ontology (GO) enrichment analysis of the hits that localize to the mitochondria indicate that mitochondrial translation is a common function for many of these genes. FDR, false discovery rate. (B) The sgRNA counts from the live cell screen for two components of the mitochondrial ribosome, MRPS39 and MRPL40, are depleted relative to counts in uninfected cells when compared with nontargeting controls. (C) sgRNA counts from the dead cell screen for three components of the mitochondrial ribosome are enriched in the KSHV-infected cells relative to the uninfected controls when compared with the nontargeting controls. (D) Western blot showing suppression of protein expression with sgRNAs targeting MRPS34 as well as a nontargeting control (NTC) sgRNA. The separate sgRNAs targeting MRPS34 are able to knock out (KO) the gene in a portion of transduced TIME cells and significantly reduce cell growth relative to mock infection when compared with nontargeting control transduced cells (paired *t* test; *n* = 4). **P* < 0.05.

to the mitochondria (shown in red in Fig. 1*B*). This represents an enrichment from 6% of the total nuclear genes whose products localize to the mitochondria. The largest subset of mitochondrial genes identified in the screen has functions in mitochondrial translation and respiration (Fig. 2*A*). The mitochondrial ribosomal subunits MRPS39 and MRPL40 had mean counts roughly four times lower in the KSHV-infected population relative to the uninfected control in the live cell screen (Fig. 2*B*). The mitochondrial ribosomal subunits MRPS34, MRPL20, and MRPL41 were counted in our dead cell screen while having little to no counts in our mock infected population (Fig. 2*C*). In an independent set of experiments, two sgRNAs targeting MRPS34 were able to moderately reduce expression of MRPS34 when visualized by western blot (Fig. 2*D*). These MRPS34 knockout cells showed reduced proliferation compared with nontargeting

control sgRNA transduced cells from 48 to 72 h postinfection (Fig. 2*D*). Knockout of MRPS34 led to the suppression of the mitochondrial genome encoded COXII (*SI Appendix, Fig. S2*). Overall, the screen implicated mitochondrial translation as a potential vulnerability, which can be used to inhibit the proliferation and survival of latently infected TIME cells.

Antibiotics Interfere with Proliferation and Survival of KSHV-Infected Cells. Since mitochondrial ribosomes are structurally more closely related to bacterial ribosomes than eukaryotic ribosomes, antibiotics that target bacterial ribosomes can be used to selectively inhibit mitochondrial translation (13). To test if antibiotics that inhibit mitochondrial translation also inhibit cells latently infected with KSHV, chloramphenicol, which interferes with the large mitochondrial ribosomal subunit,

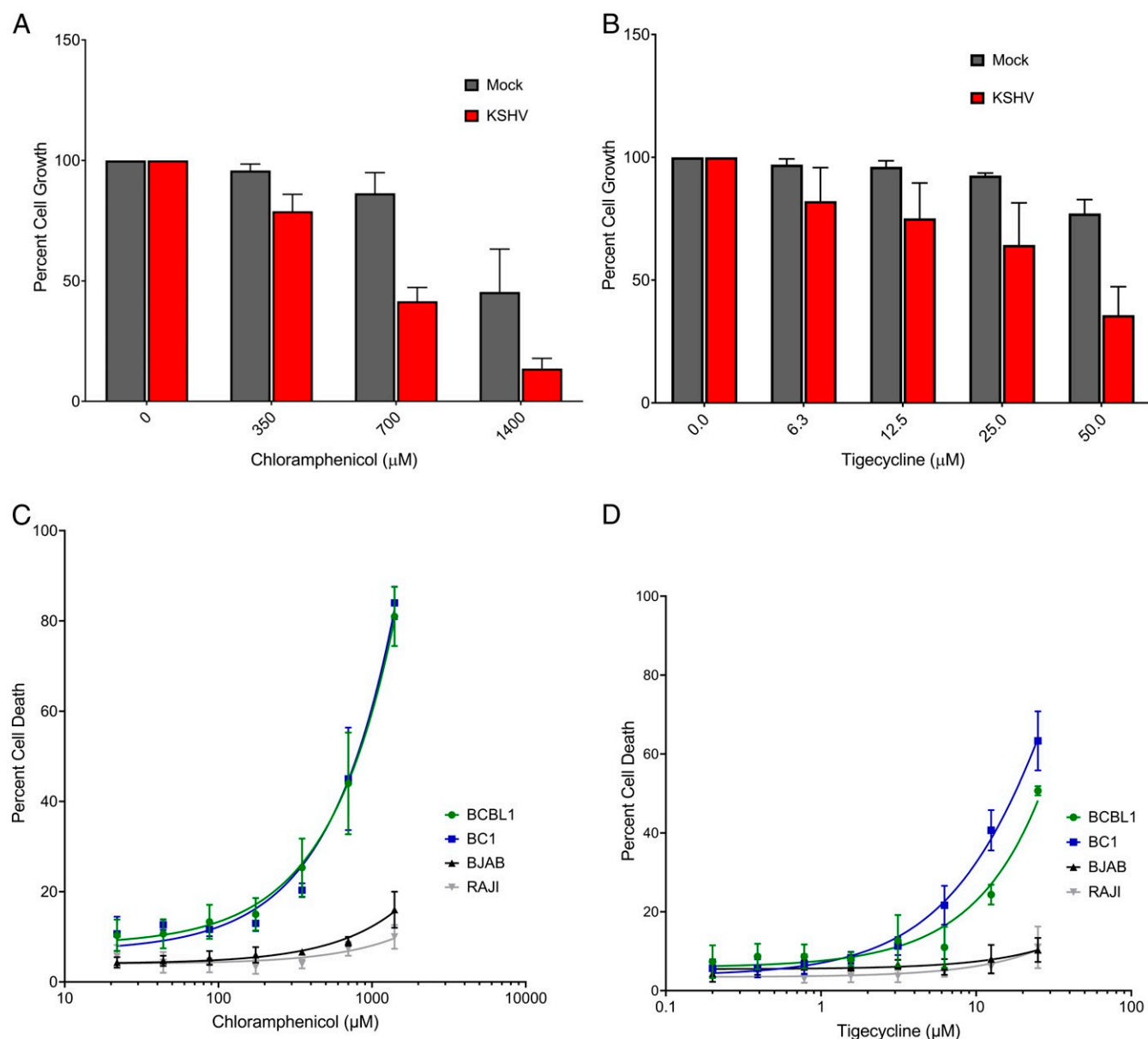


Fig. 3. Antibiotics targeting bacterial translation inhibit the growth and survival of cells latently infected with KSHV. Treatment of KSHV-infected TIME cells suppresses cell growth in a dose-dependent manner with both chloramphenicol (*A*) and tigecycline (*B*; mean with SEM of three replicate experiments). KSHV-infected PEL, BCBL1 and AIDS body cavity-based lymphoma 1 (BC1), cells exhibit a dose-dependent induction of cell death for both chloramphenicol (*C*) and tigecycline (*D*), which is not seen in B cell lymphomas lacking KSHV (the EBV negative Burkitt's lymphoma BJAB, and the EBV positive Burkitt's lymphoma RAJI).

and tigecycline, which inhibits the small subunit, were used to treat latently infected cells. KSHV-infected TIME cells showed a dose-dependent decrease in cell confluence relative to mock infected controls for both chloramphenicol (Fig. 3A) and tigecycline (Fig. 3B) after 48 h of treatment. Therefore, treatment of infected TIME cells with tigecycline or chloramphenicol leads to an inhibition of cell expansion. To determine if this sensitivity is unique to infected endothelial cells, KSHV-negative and KSHV-positive B cell lymphomas were also tested for sensitivity. KSHV-positive B cells show a dose-dependent sensitivity to treatment with either antibiotic at 48 h posttreatment (Fig. 3C and D). All B cell lymphomas tested exhibited dose-dependent inhibition of cellular proliferation in response to antibiotic treatment; however, KSHV-infected PEL cells were more sensitive than lymphomas lacking KSHV (*SI Appendix*, Fig. S3).

Mitochondrial Respiratory Function Is an Essential Process during Latent KSHV Infection. If suppression of mitochondrial translation is essential due to the loss of expression of respiratory complex components, then inhibitors of respiration should also lead to increased cell death and decreased proliferation in KSHV-infected cells. This hypothesis is supported by the presence of mitochondrial genes among the previously discovered PEL-specific oncogenic dependencies (10). KSHV-infected TIME cells were treated with the complex I inhibitor rotenone but showed no difference in cellular proliferation when compared with uninfected controls (*SI Appendix*, Fig. S4). However, endothelial cell media contain pyruvate, which is known to rescue cells from rotenone sensitivity, and there is no available pyruvate-free endothelial media (14). Therefore, we tested KSHV-infected PEL cells in media lacking pyruvate and found a dose-dependent increase in cell death (Fig. 4A), similar to the increase in cell death from chloramphenicol and tigecycline treatment. We attempted to rescue rotenone-induced cell death in PEL cells with pyruvate; however, we did not observe a reduction in cell death with either 1 or 10 mM pyruvate added to the media (*SI Appendix*, Fig. S5). It is unclear if the difference between the cell types is dependent on differences in the media or due to cell-intrinsic factors. As an alternative way to test for the essentiality of respiration during KSHV infection of endothelial cells, mitochondrial genomes were eliminated from TIME cells using a genetic, inducible mutagenesis system (15). This system uses a mutant uracil *N*-glycosylase, which removes thymine from DNA. This enzyme has a mitochondrial targeting sequence and is placed under the control of a tet-inducible promoter. As a control, the wild-type enzyme wild-type uracil *N*-glycosylase, which can only remove uracil from RNA, is placed in an identical expression system. After 2 weeks of induction, cells were removed from doxycycline, and loss of expression of the mitochondrial genome encoded COXII, as well as the expected loss of expression of some nuclear-encoded mitochondrial genes due to decreased complex stability (16), was confirmed by western blot (*SI Appendix*, Fig. S6A). Cell proliferation was compared between cells with intact mitochondria and those without functioning mitochondrial genomes in both the presence and absence of KSHV infection. Cells were plated to 24-well plates and imaged on an Incucyte for 6 d with media changes every 2 d. The resulting curves show that depletion of mitochondrial genomes leads to a decrease in proliferation during KSHV infection (Fig. 4B) and an increase in log phase doubling time (*SI Appendix*, Fig. S6B). Additionally, KSHV infection selectively induces death in cells lacking functional mitochondria when compared with mock infected controls (Fig. 4C). Taken together, these results show that inhibitors of respiration or elimination of functional mitochondrial genomes from cells lead to inhibition of cellular proliferation in the case of TIME cells and induction of cell death in KSHV-infected PEL cells. These results suggest that mitochondrial respiration is required

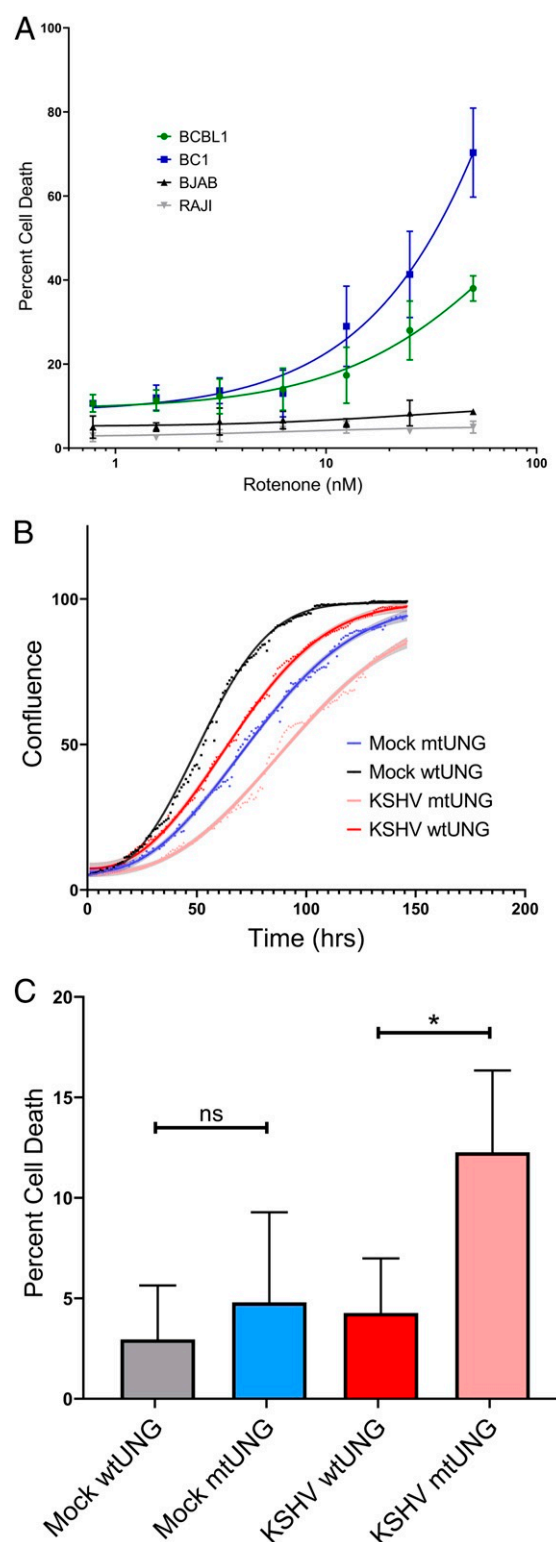


Fig. 4. Inhibition of respiration or loss of mitochondrial genomes suppresses proliferation and survival of KSHV-infected cells. (A) Rotenones induces cell death in PEL cells in a dose-dependent manner, while BJAB and RAJI cells show no sensitivity at the tested concentrations. (B) After ablation of functional mitochondrial genomes, KSHV-infected cells lacking mitochondria grow at a slower rate when compared with mock infected cells lacking mitochondria. (C) Additionally, KSHV-infected cells lacking mitochondria show an induction in cell death upon infection relative to controls (paired *t* test; *n* = 3). mtUNG, mutant uracil *N*-glycosylase; wtUNG, wild-type uracil *N*-glycosylase. **P* < 0.05; ns, nonsignificant.

for the proliferation and survival of cells latently infected with KSHV.

Latent KSHV Infection Increases Mitochondrial Transcripts and Genome Copy Number. Previous work from our laboratory established that mitochondrial function is decreased during KSHV infection (4). One possible explanation that is consistent with both the decreased mitochondrial function and sensitivity to antibiotic treatment is that mitochondria are physically defective in cells latently infected with KSHV. Defects in mitochondrial function can lead to a fragmented mitochondrial network, which is a previously observed characteristic of certain cancers exhibiting Warburg metabolism (17). To better characterize the state of the mitochondrial network during KSHV infection, KSHV-infected and mock infected endothelial cells were fixed to slides and probed for COXIV as a marker for mitochondria. Images were analyzed using an ImageJ plug-in for examining mitochondrial networks (18). There was a decrease in the average number of mitochondria per cell (effect size of 47.9) and increases in the average size and length of mitochondria (effect sizes of 38.6 and 25.1% in KSHV-infected cells relative to mock cells, respectively) (Fig. 5A–C).

Mitochondrial function can be altered at the level of mitochondrial gene transcription. Our previously published RNA-sequencing dataset (7) was analyzed to look at average gene expression across each chromosome, including the mitochondrial chromosome. While the mean change in transcript level for all genes on a given chromosome was near zero for every nuclear chromosome, the mitochondrial genome showed a 1.29-fold average increase during KSHV infection (*SI Appendix, Fig. S7A*).

This increase in expression is primarily from transfer RNAs (*SI Appendix, Fig. S7B*), which are the only transcripts stabilized by polyadenylation in mitochondria, and our complementary DNA library was poly-deoxythymidine primed. To confirm that transcription of the entire mitochondrial genome is increased during KSHV infection, qRT-PCR primed with random primers showed that transcripts of both strands of the mitochondrial genome are increased during KSHV infection (Fig. 5D). To determine if this increase in transcript levels was related to genome copy number, qPCR of mitochondrial genome copy number showed that KSHV-infected TIME cells possess approximately twice as many mitochondrial genomes as mock infected cells (Fig. 5E). Overall, KSHV infection of TIME cells leads to an increase in the size, length, transcript levels, and genome copies per cell of mitochondria while decreasing the overall number of mitochondria. These results are consistent with increased mitochondrial fusion during KSHV infection, rather than defective mitochondria. The reduction in oxygen consumption observed during KSHV infection is independent of mitochondrial network structure, mitochondrial transcription, and mitochondrial genome copy number.

KSHV Latency Gene Products Localize to Mitochondrial Fractions.

To determine if any KSHV latent genes could play a direct role in the alteration of mitochondrial biology, the localization of latent proteins to the mitochondria was examined. Plasmids for transient overexpression of each of the latent proteins with 3xFLAG tag on the N-terminal end were transfected into 293T cells; 48 h later, the cytoplasmic and mitochondrial fractions of the cells were separated using differential centrifugation. Western blot analysis of whole-cell lysates and the mitochondrial and

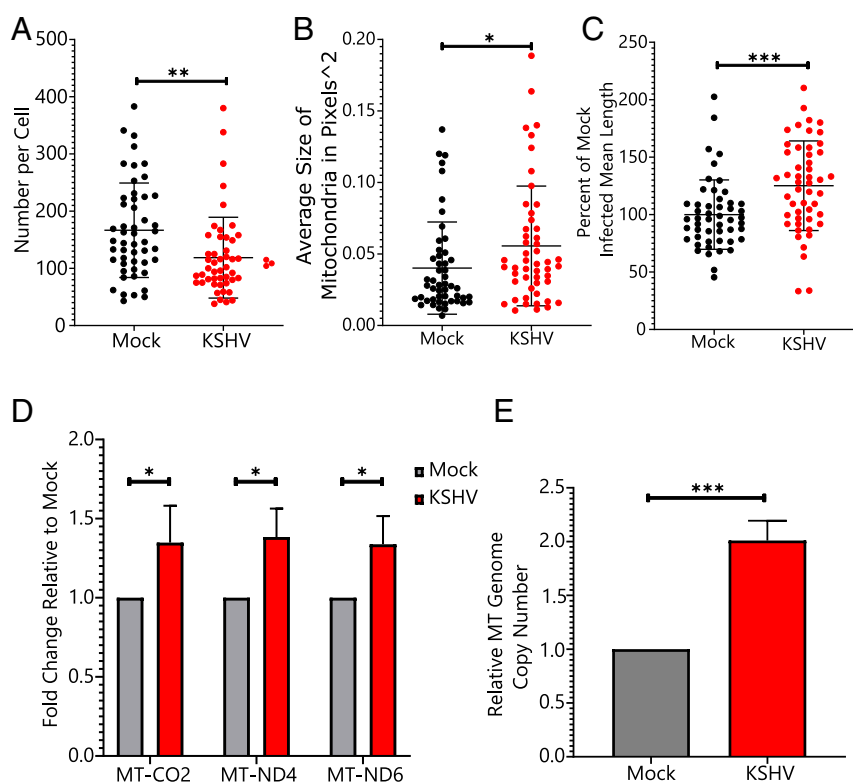


Fig. 5. KSHV infection induces changes in the mitochondrial network and increases mitochondrial transcription and genome copy number. KSHV-infected cells were analyzed by immunofluorescence for changes in the mitochondrial network in single cells. The average mitochondrial number decreased per cell (A), while the average area (B) and length (C) of mitochondria increased (unpaired *t* test; *n* = 50 per sample). **P* < 0.05; ***P* < 0.01; ****P* < 0.001. (D) qRT-PCR shows that transcript levels from the mitochondrial (MT) genome increase during KSHV infection (paired *t* test; *n* = 3). **P* < 0.05. (E) qPCR for mitochondrial genome copies relative to host genome copies shows an increase in mitochondrial genome copy number during KSHV infection of TIME cells (paired *t* test; *n* = 6). ****P* < 0.001.

cytoplasmic fractions of the cells was used to identify localization of the viral proteins. Glyceraldehyde 3-phosphate dehydrogenase (GAPDH) was used as a marker for the cytoplasmic fraction, and ATP5A was used as a marker for the mitochondria. Kaposin B (KapB) was present at low levels in the mitochondrial fraction as well as the cytoplasmic fraction, and a small portion of the viral cyclin (vCyc) was also present in the mitochondrial fraction. The viral FLICE-inhibitory protein (vFLIP) construct with an N-terminal tag could not be detected. However, a lentiviral-based vector with a C-terminal V5 tag was detected and indicated a proportion of vFLIP localizes to the mitochondrial fraction.

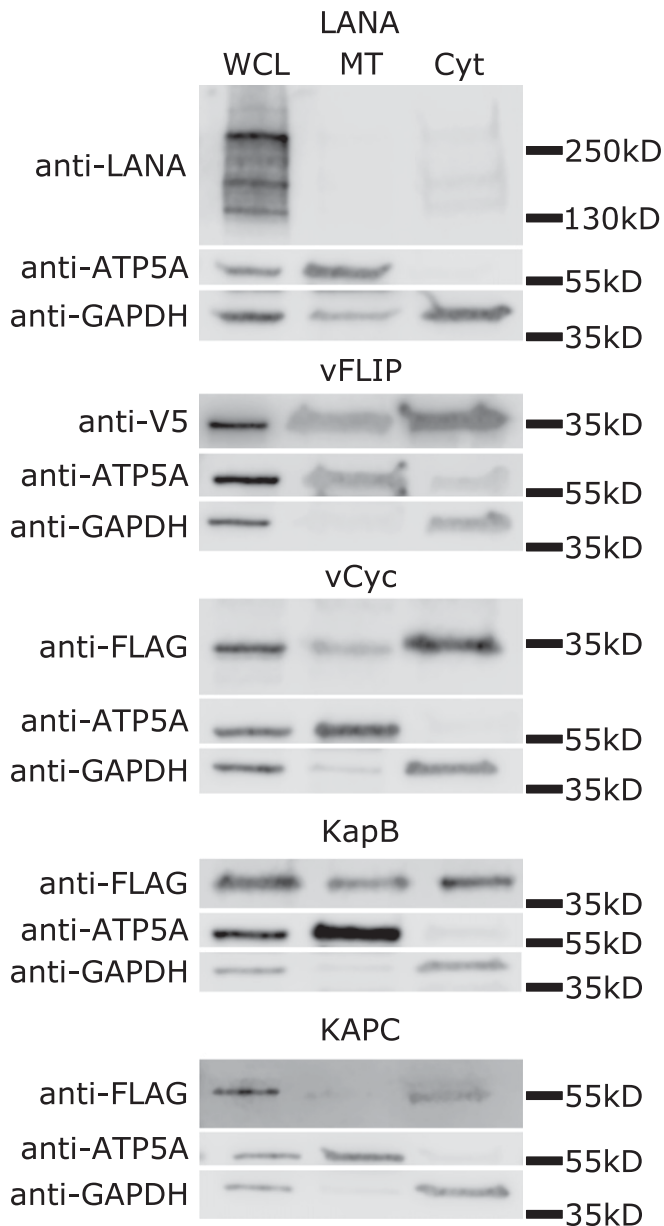


Fig. 6. KSHV latent proteins localize to the mitochondrial fraction. Mitochondrial fractionation by differential centrifugation was used to separate cytosolic and mitochondrial fractions of 293T cells 48 h after transfection (in the case of all but vFLIP, where lentivirus transduction was used). Whole-cell lysates (WCL) were run along with the reduced cytosolic (Cyt) and mitochondrial (MT) fractions. Blots were probed for the indicated tag depending on the construct as well as ATP5A and GAPDH. vCyc, vFLIP, and Kaposin B (KapB) are partially localized to the mitochondria, while LANA and Kaposin C (KapC) are absent.

Kaposin C (KapC) and LANA did not display localization to the mitochondrial fraction (Fig. 6). The presence of multiple latent genes in the mitochondrial fraction is consistent with the idea that the virus might be directly interfering with mitochondrial function during latent infection.

Discussion

While traditional chemotherapies and newer personalized medical approaches have improved clinical outcomes for KS in the developed world, cost and availability limit their utility in developing countries (1). As KS is the third most common cancer in sub-Saharan Africa, there is a need for readily available therapies. Whole-genome essentiality screens have already been applied to a number of different cancers as well as pathogen infections. These screens have proven to be a powerful source of potential therapeutic targets in preclinical work. We used CRISPR-Cas9 lentiviral library screening to identify cellular genes whose function is essential for the survival of human endothelial cells latently infected with KSHV, the cell type most relevant for KS spindle cells. We found 146 potential targets in our initial whole-genome screen, a number of which can be targeted with approved drugs or drugs that are in clinical trials.

A large number of genes identified by the screen encode proteins that localize to the mitochondria, leading to the hypothesis that mitochondrial translation is essential for proliferation or survival of cells latently infected with KSHV. Mitochondrial ribosomes can be targeted therapeutically using antibiotics due to the shared ancestry between bacterial ribosomes and eukaryotic mitochondrial ribosomes. This aspect of mitochondrial biology has been exploited for other cancers (19–22). Importantly, many of these antibiotics are readily available and on the World Health Organization List of Essential Medicines (23). We showed that both chloramphenicol and tigecycline are able to suppress proliferation of infected endothelial cells and induce cell death in KSHV-infected B cells. Since the mitochondrial ribosome is primarily responsible for synthesizing components of the respiratory chain, our findings suggest that KSHV-infected cells require some mitochondrial function despite having lower basal levels of mitochondrial function. Our live cell screen dataset contains three hits common to the list of PEL-specific oncogenic dependencies from a CRISPR-Cas9 screen done in KSHV-positive B cell lymphoma cell lines (10). These three genes, NDUFB7, PTC3, and TAZ, localize to the mitochondria and form part of respiratory complex I, the small mitochondrial ribosomal subunit, and the mitochondrial protein import machinery, respectively. Interestingly, while antibiotics inhibited both endothelial cells latently infected with KSHV and PEL cells, there were slightly different outcomes. The infected endothelial cells were unable to reach confluence as quickly as mock infected controls, but there was not obvious large-scale cell death, while in the PEL cells, there was widespread cell death. The mechanistic reason for the difference in responses between cell types is currently unclear.

We and others have shown that KSHV-infected cells display characteristics of Warburg metabolism (4, 24–26). This includes increased glucose consumption, increased production of lactate, and decreased oxygen consumption (27). This collection of phenotypes is consistent with the presence of mitochondrial defects within cells, which is an observation made by Otto Warburg himself (28). We sought to confirm the presence of mitochondrial defects by looking for changes in mitochondrial network structure, transcript levels, genome copy number, and protein levels in infected endothelial cells. However, the changes we observed in network structure, transcripts, and genomes were not consistent with mitochondrial dysfunction, which usually produces fractured mitochondrial networks, fewer genomes, and lower RNA levels (29, 30). Interestingly, despite the increase in mitochondrial DNA copy number and transcript levels, there was a decrease in overall mitochondrial number in latently infected endothelial

cells. At the same time, there was an increase in mitochondrial size. These results are consistent with, but not definitive proof of, increased mitochondrial fusion. Further experiments will be needed to examine changes in mitochondrial fusion dynamics during KSHV infection and determine the role latent genes might be playing to facilitate or counteract mitochondrial changes during latent infection of human endothelial cells.

Many viruses encode proteins, which modify mitochondrial function for a variety of different reasons. Among the observed functions are preventing apoptosis, inducing changes in metabolism, and avoiding innate immune activation. Some viruses encode proteins, which have been found to interact with mitochondrial ribosomes in large-scale protein interaction studies. These include the capsid proteins of flaviviruses (31) and Nsp8 of the severe acute respiratory syndrome coronavirus-2 (32). A previously published KSHV protein interaction network identified potential interactions between KSHV latent genes and mitochondrial proteins (33). Ninety-two mitochondrial genes were within vFLIP's interaction network, representing 19.1% of all proteins in the interaction network; 5% of vFLIP's interaction network is made up of proteins involved in mitochondrial translation. Consistent with these findings, we found that vFLIP physically localizes to the mitochondria. Further studies examining the direct effects of viral proteins in the mitochondria will be necessary to determine the mechanism of KSHV alteration of mitochondrial biology.

Whole-genome screening for factors that are essential to latent KSHV infection led us to unexplored therapeutic targets and pointed us toward an additional point of viral interaction with the host cell. While KS is a multifactorial disease, the fact that the proliferating component is a latently infected endothelial cell has prevented direct targeting of the viral infection. Identifying host genes whose inhibition can selectively eliminate KSHV-infected cells has potential for application in the clinic. While previous work has demonstrated that specific metabolic processes can be used to kill latently infected cells, the central nature of many of those metabolic pathways limits their utility. A narrowing of the target range to even more specific cellular pathways can make a therapeutic more attractive than broad metabolic inhibitors. While mitochondrial translation is an intriguing target, the concentrations of antibiotics used in this study to inhibit KSHV-infected cell proliferation were relatively high. Future work will determine if antibiotic combinations or other antibiotics known to target the mitochondria better than chloramphenicol and tigecycline could identify effective treatments at more reasonable concentrations of antibiotic. While targeting mitochondrial translation is likely still problematic, this work encompasses a step toward gaining a better understanding of viral alteration of a cellular metabolic hub, which can then enable targeting more precise pathways.

Datasets. Gene scores and sgRNA counts from the live and dead cell screens can be found in [Datasets S1](#) (live cell screen) and [S2](#) (dead cell screen). [SI Appendix, Figs. S1–S5](#) as well as materials tables for antibodies, primers, and plasmids can be found in [SI Appendix](#). Raw sequencing data are available at Gene Expression Omnibus (GEO) accession number [GSE152284](#) (34).

Materials and Methods

Cell Lines. TIME cells were maintained in endothelial cell basal medium-2 (EBM-2) media (Lonza), which was supplemented with an EGM-2 MV SingleQuot Microvascular Endothelial Cell Growth Medium Bullet Kit (Lonza) containing 5% fetal bovine serum (FBS), hydrocortisone, hFGF-B, VEGF, R3-IGF-1, ascorbic acid, and hEGF, as well as gentamycin and amphotericin-B. After the screen was performed, we discovered the presence of *Mycoplasma arginini* in TIME cells. The Plasmotest mycoplasma detection kit (Invivogen) was used to find that TIME cells test positive for mycoplasma after a minimum of 72 h of growth in the absence of antibiotic. This was confirmed by performing a genomic DNA extraction using the PureLink Genomic

DNA Mini Kit (Invitrogen) followed by the LookOut *Mycoplasma* Detection Kit (Sigma-Aldrich); 293 and 293T cells were grown in Dulbecco's modified Eagle media (DMEM) (+L-glutamine, +penicillin-streptomycin, +4.5g/L glucose, +sodium pyruvate, + 10% FBS; Fisher). B cell lymphomas were grown in Roswell Park Memorial Institute media (RPMI) 1640 (+L-glutamine, +penicillin-streptomycin, + 2-mercaptoethanol, + 10% FBS; Fisher). iSLK cells for BAC16 virus production were grown in DMEM (+L-glutamine, +penicillin-streptomycin, +4.5g/L glucose, +sodium pyruvate, + 10% FBS). All 293T cells, B cell lymphomas, iSLK cells, and the mitochondria lacking TIME cells in Fig. 4 B and C were negative for mycoplasma by both the Invivogen and Invitrogen kits listed above.

Transfection. The 293T cells were seeded at 10,000 cells per centimeter² the night before transfection. Transit 293T (Mirus Bio) was used to transfect plasmids as indicated by the manufacturer. After 24 h, the media on the cells were replaced with fresh serum containing media. In the case of lentivirus production, the masses of each plasmid used were 8 µg of pSPAX2, 4 µg of pMD2.G, and 8 µg of the lentiviral vector. Culture supernatants were collected at 48 and 72 h posttransfection and filtered through 0.45-µm filters before aliquoting and freezing.

Proliferation Assay. Time cells were seeded at 1×10^4 cells per centimeter² and then treated once settled. After the specified length of time, when assessing cell death, the time cells were treated with trypsin and counted after trypan blue staining for cell viability. When assessing cell proliferation, TIME cells were washed twice with phosphate buffered saline (PBS) and fixed with 100% methanol. After fixing, the cells were stained with crystal violet for 10 min and then rinsed with distilled water until dye no longer washed off. The plates are allowed to dry overnight before scanning with a Typhoon imager (GE) using a 532-nm laser and a 670BP30 filter. The resulting images were analyzed in ImageJ to measure cell confluence in each well. The MRP534 data in Fig. 2 were obtained by resuspending the crystal violet with 500 µL 10% glacial acetic acid after staining and measuring 200 µL of the resulting solution in a 96-well plate reader at 570 nm. All transformed B cell proliferation assays began with viable cell concentrations of 2×10^5 . Forty-eight hours after treatment, cells were stained with trypan blue and counted using a TC-20 Cell Counter (BioRad).

qRT-PCR. Cell lysates were harvested using Nucleospin RNA II Kits (Macherey Nagel). RNA was quantified by Nanodrop, and the quality of each sample was assessed on a 1% agarose gel in Tris-acetate-ethylenediaminetetraacetic acid (EDTA) buffer to ensure that no degradation of samples had occurred; 500 ng of RNA was used for each 20-µL reverse transcription reaction with the iScript Select cDNA Synthesis Kit (BioRad) using random primers. qPCR was subsequently carried out using SsoAdvanced Universal SYBR Green Supermix (BioRad). Primers targeting hypoxanthine-guanine phosphoribosyltransferase (HPRT) were used as a reference, and primers targeting mitochondrial genome sequences were used to assess transcript levels. Primer sequences are available in [SI Appendix, Table S5](#).

qPCR for Mitochondrial Genome Quantitation. Cell lysates were harvested using PureLink Genomic DNA Mini Kits (Invitrogen). The resulting genomic DNA is used as template for qPCR with SsoAdvanced Universal SYBR Green Supermix (BioRad). Primers targeting Prox1 were used as a reference for cellular genomic DNA, and primers targeting the mitochondrial genome were used to quantify mitochondrial genome copy number. Primer sequences are available in [SI Appendix, Table S5](#).

CRISPR-Cas9 Whole-Genome Library. One-half of the Human Activity-Optimized CRISPR Knockout Library was transformed into Endura electrocompetent cells (Lucigen). Sufficient colony-forming units to achieve 1,000-times coverage of the library were harvested using the Plasmid Plus Maxi Kit (Qiagen). The resulting plasmid prep was transfected into 293T cells as mentioned above for production of lentivirus. The resulting lysate was titrated onto TIME cells using cell viability after selection as a proxy for infection. Thirty-six T225s containing 4.5×10^6 TIME cells per flask seeding the evening before transduction were treated with the lentiviral library. This is roughly 150 million cells transduced at an MOI of 0.6 to achieve at least 500-times coverage of the library. Transduced time cells were selected for 3 d and grown for an additional 4 d until two sets of 34 T225s could be seeded. The day after seeding, one set of the TIME cells was infected with KSHV purified from BCBL1 cells as previously described (35). Two days after infection, the TIME cells were split and infected again. The infection rates for the cells were counted by immunofluorescence for LANA and open reading frame 59. For the next 8 d, the cells were split every 2 d and reseeded to 4.5

million TIME cells per flask, maintaining 34 flasks for each sample. At each passage, the culture supernatants were collected, and dead cell pellets were frozen after centrifugation. At the end of the experiment, all live cells were collected, and dead cell samples were pooled for uninfected and infected cells. Genomic DNA was harvested from all samples using the blood and cell culture DNA maxi kit (Qiagen). The genomic DNA was used as template for Illumina sequencing amplicons as described in Wang et al. (8).

Analysis of CRISPR-Cas9 Library Screening. Illumina sequencing results were analyzed using MAGeCK version 5.6 (12). sgRNAs were counted after deconvolution of samples, allowing for up to one uncalled base per guide. The live cell screen was analyzed using uninfected as the control and KSHV-infected TIME cells as the treatment group. The sgRNA counts were normalized based on median read counts, and the distribution of nontargeting sgRNAs was used to generate the null distribution. The dead cell sequencing results were analyzed in an identical manner, except the sgRNA counts were normalized based on total read counts. All other parameters used the default settings for MAGeCK.

Western Blot Analysis. Cells were harvested using trypsin to remove adherent cells and then pelleted and washed once with PBS. Cell pellets were lysed with radioimmunoprecipitation assay (RIPA) buffer (50 mM Tris-HCl, pH 7.6, 150 mM NaCl, 1 mM EDTA, 1% Nonidet P-40, 0.5% deoxycholate, 0.1% sodium dodecyl sulfate, 1 mM sodium orthovanadate, 1 mM sodium fluoride, 40 mM β -glycerophosphate, Complete Mini protease inhibitor tablet; Roche). Cell lysate was quantified using the Peirce BCA assay (ThermoFisher Scientific), and equal masses of protein were loaded to a 4 to 20% polyacrylamide gel (BioRad). The protein was transferred to a polyvinylidene difluoride membrane and blotted using the appropriate primary antibody at the dilutions mentioned above. Blots were treated with LI-COR IRDye secondary antibodies prior to imaging on either a LI-COR Odyssey CLx or Odyssey Fc system.

Mitochondrial Immunofluorescence. TIME cells were fixed to glass chamber well slides with 4% paraformaldehyde. After blocking and probing with an

anti-COXIV primary antibody and fluorescent secondary antibodies, the cells were mounted with Vectashield mounting medium with 4',6-diamidino-2-phenylindole (Vector Laboratories). Images were captured using a Retiga R6 camera (Teledyne Photometrics). Images were analyzed in FIJI (36) using macros adapted from ref. 18. Resulting outputs for mitochondrial number, average length, and total volume were quantified per cell and plotted in PRISM8 (Graphpad Software).

Mitochondrial Fractionation. Cell pellets were resuspended in PBS and processed using the Mitochondria Isolation Kit for Cultured Cells (ThermoFisher Scientific). The manufacturer's recommendations were followed to achieve a high-purity mitochondrial fraction through differential centrifugation, which after purification, was lysed with RIPA buffer. Protein concentrations of the resulting lysate, paired cytoplasmic fraction, and whole-cell lysate were quantified, and equal masses of each fraction were processed as previously mentioned. To check the validity of the purification, blots were probed with primary antibodies targeting five mitochondrial proteins to confirm enrichment and GAPDH to check for cytoplasmic contamination of the mitochondrial fraction.

Data Availability. Gene scores and sgRNA counts from the live and dead cell screens can be found in [Datasets S1](#) (live cell screen) and [S2](#) (dead cell screen). [SI Appendix, Figs. S1–S5](#) as well as materials tables for antibodies, primers, and plasmids can be found in [SI Appendix](#). Screen next generation sequencing results data have been deposited in the GEO (GSE152284).

ACKNOWLEDGMENTS. D.L.H. was supported in part by National Institute of Allergy and Infectious Diseases of the NIH Training Grant T32AI083203. This work was supported by National Cancer Institute Grants RO1CA189986 (to M.L.), RO1CA217788 (to M.L.), and R21CA240479 (to M.L.). We thank the Fred Hutchinson Cancer Research Center genomics core for performing the Illumina deep sequencing and members of the laboratory of M.L. for advice and discussion over the course of the project. We also thank Terri DiMaio for advice and editing during the preparation of the manuscript. The funders had no role in study design, data collection and analysis, decision to publish, or preparation of the manuscript.

1. E. Cesarman et al., Kaposi sarcoma. *Nat. Rev. Dis. Primers* **5**, 9 (2019).
2. W. Zhong, H. Wang, B. Herndier, D. Ganem, Restricted expression of Kaposi sarcoma-associated herpesvirus (human herpesvirus 8) genes in Kaposi sarcoma. *Proc. Natl. Acad. Sci. U.S.A.* **93**, 6641–6646 (1996).
3. M. Lagunoff et al., De novo infection and serial transmission of Kaposi's sarcoma-associated herpesvirus in cultured endothelial cells. *J. Virol.* **76**, 2440–2448 (2002).
4. T. Delgado et al., Induction of the Warburg effect by Kaposi's sarcoma herpesvirus is required for the maintenance of latently infected endothelial cells. *Proc. Natl. Acad. Sci. U.S.A.* **107**, 10696–10701 (2010).
5. T. Delgado, E. L. Sanchez, C. Roman, M. Lagunoff, Global metabolic profiling of infection by an oncogenic virus: KSHV induces and requires lipogenesis for survival of latent infection. *PLoS Pathog.* **8**, e1002866 (2012).
6. E. L. Sanchez, P. A. Carroll, A. B. Thalhoffer, M. Lagunoff, Latent KSHV infected endothelial cells are glutamine addicted and require glutaminolysis for survival. *PLoS Pathog.* **11**, e1005052 (2015).
7. Z. E. Sychev et al., Integrated systems biology analysis of KSHV latent infection reveals viral induction and reliance on peroxisome mediated lipid metabolism. *PLoS Pathog.* **13**, e1006256 (2017).
8. T. Wang, J. J. Wei, D. M. Sabatini, E. S. Lander, Genetic screens in human cells using the CRISPR-Cas9 system. *Science* **343**, 80–84 (2014).
9. Y. Ma et al., CRISPR/Cas9 screens reveal Epstein-Barr virus-transformed B cell host dependency factors. *Cell Host Microbe* **21**, 488–499 (2013).
10. M. Manzano et al., Gene essentiality landscape and druggable oncogenic dependencies in herpesviral primary effusion lymphoma. *Nat. Commun.* **9**, 3263 (2018).
11. M. Gruffaz et al., CRISPR-Cas9 screening of Kaposi's sarcoma-associated herpesvirus-transformed cells identifies XPO1 as a vulnerable target of cancer cells. *mBio* **10**, e00866 (2019).
12. W. Li et al., MAGeCK enables robust identification of essential genes from genome-scale CRISPR/Cas9 knockout screens. *Genome Biol.* **15**, 554 (2014).
13. B. H. Cohen, R. P. Saneto, Mitochondrial translational inhibitors in the pharmacopeia. *Biochim. Biophys. Acta* **1819**, 1067–1074 (2012).
14. M. P. King, G. Attardi, Human cells lacking mtDNA: Repopulation with exogenous mitochondria by complementation. *Science* **246**, 500–503 (1989).
15. I. N. Shokolenko, G. L. Wilson, M. F. Alexeyev, Persistent damage induces mitochondrial DNA degradation. *DNA Repair* **12**, 488–499 (2013).
16. J. Rusecka, M. Kaliszewska, E. Bartnik, K. Tońska, Nuclear genes involved in mitochondrial diseases caused by instability of mitochondrial DNA. *J. Appl. Genet.* **59**, 43–57 (2018).
17. A.-H. Giang et al., Mitochondrial dysfunction and permeability transition in osteosarcoma cells showing the Warburg effect. *J. Biol. Chem.* **288**, 33303–33311 (2013).
18. R. A. Merrill, K. H. Flippo, S. Strack, "Measuring mitochondrial shape with ImageJ" in *Techniques to Investigate Mitochondrial Function in Neurons*, S. Strack, Y. Usachev, Eds. (Neuromethods, Humana Press, New York, NY, 2017), vol. 123, pp. 31–48.
19. S. Kalghatgi et al., Bactericidal antibiotics induce mitochondrial dysfunction and oxidative damage in mammalian cells. *Sci. Transl. Med.* **5**, 192ra85 (2013).
20. R. Lamb et al., Antibiotics that target mitochondria effectively eradicate cancer stem cells, across multiple tumor types: Treating cancer like an infectious disease. *Oncotarget* **6**, 4569–4584 (2015).
21. M. Škrčić et al., Inhibition of mitochondrial translation as a therapeutic strategy for human acute myeloid leukemia. *Cancer Cell* **20**, 674–688 (2011).
22. J. Tan, M. Song, M. Zhou, Y. Hu, Antibiotic tigecycline enhances cisplatin activity against human hepatocellular carcinoma through inducing mitochondrial dysfunction and oxidative damage. *Biochem. Biophys. Res. Commun.* **483**, 17–23 (2017).
23. World Health Organization, "Executive summary: The selection and use of essential medicines 2019: Report of the 22nd WHO Expert Committee on the selection and use of essential medicines" (Rep.WHO/MVP/EMP/IAU/2019.05, World Health Organization, 2019; <https://www.who.int/publications/i/item/executive-summary-the-selection-and-use-of-essential-medicines-2019-report-of-the-22nd-who-expert-committee-on-the-selection-and-use-of-essential-medicines>).
24. A. P. Bhatt et al., Dysregulation of fatty acid synthesis and glycolysis in non-Hodgkin lymphoma. *Proc. Natl. Acad. Sci. U.S.A.* **109**, 11818–11823 (2012).
25. O. Yogev, D. Lagos, T. Enver, C. Boshoff, Kaposi's sarcoma herpesvirus microRNAs induce metabolic transformation of infected cells. *PLoS Pathog.* **10**, e1004400 (2014).
26. T. Ma et al., KSHV induces aerobic glycolysis and angiogenesis through HIF-1-dependent upregulation of pyruvate kinase 2 in Kaposi's sarcoma. *Angiogenesis* **18**, 477–488 (2015).
27. O. Warburg, F. Wind, E. Negelein, The metabolism of tumors in the body. *J. Gen. Physiol.* **8**, 519–530 (1927).
28. O. Warburg, On the origin of cancer cells. *Science* **123**, 309–314 (1956).
29. A. Trifunovic et al., Premature ageing in mice expressing defective mitochondrial DNA polymerase. *Nature* **429**, 417–423 (2004).
30. J. Nunnari, A. Suomalainen, Mitochondria: In sickness and in health. *Cell* **148**, 1145–1159 (2012).
31. P. S. Shah et al., Comparative flavivirus-host protein interaction mapping reveals mechanisms of dengue and Zika virus pathogenesis. *Cell* **175**, 1931–1945.e18 (2018).
32. D. E. Gordon et al., A SARS-CoV-2 protein interaction map reveals targets for drug repurposing. *Nature* **583**, 459–468 (2020).
33. Z. H. Davis et al., Global mapping of herpesvirus-host protein complexes reveals a transcription strategy for late genes. *Mol. Cell* **57**, 349–360 (2015).
34. R. Edgar, M. Domrachev, A. E. Lash, Gene Expression Omnibus: NCBI gene expression and hybridization array data repository. *Nucleic Acids Res.* **30**, 207–210 (2002).
35. A. S. Punjabi et al., Persistent activation of STAT3 by latent Kaposi's sarcoma-associated herpesvirus infection of endothelial cells. *J. Virol.* **81**, 2449–2458 (2007).
36. S. Johannes et al., Fiji: An open-source platform for biological-image analysis. *Nat. Methods* **9**, 676–682 (2012).